ELSEVIER

Journal of Alloys and Compounds 281 (1998) 17–22

Journal of ALLOYS AND COMPOUNDS

The coercivities of nanophase melt-spun PrFeB alloys

G. Mendoza-Suárez*, H.A. Davies

Department of Engineering Materials, University of Sheffield, Mappin St., Sheffield S1 3JD, UK

Abstract

The effects of the mean $Pr_2Fe_{14}B$ crystallite size (d_g) and alloy composition on the magnetic properties of a series of nanocrystalline melt-spun $Pr_xFe_{94-x}B_6$ alloys (with $6 \leq x \leq 20$ at%) have been investigated. In all cases, the remanent polarisation J_r increases with decreasing d_g up to a maximum, at which vitrification is initiated. Except for the single phase near-stoichiometric alloy, the intrinsic coercivity also rises with decreasing d_g. The composition dependencies of J_r and ${}_jH_c$ for d_g generally in the range 20–30 nm are compared with those for corresponding NdFeB alloys. Significantly better combinations of ${}_jH_c$ and maximum energy product $(BH)_{max}$ are obtained for the PrFeB than for the NdFeB resulting from the higher anisotropy field of the $Pr_2Fe_{14}B$ phase.

Keywords: Magnetic properties; Nanocrystallite size; PrFeB alloys

1. Introduction

Hard magnetic alloys based on the compound $Nd_2Fe_{14}B$ have been extensively studied over the last 13 years and they have established a strong commercial presence in the marketplace. Among the more interesting effects, scientifically and technologically, manifested by these alloys is the phenomenon of remanence enhancement associated with refinement of the $Nd_2Fe_{14}B$ crystallites (below about 50 nm mean diameter) [1,2]. Further enhancement can be achieved through microstructural engineering of a nanocomposite structure in which crystallites of a high saturation soft magnetic phase are introduced as a second phase [3–5]. Considerable effort has been directed at characterising and understanding the enhancement effect, both through systematic experimental study [6] and through numerical modelling [7]. The studies have concentrated mainly on the NdFeB system with relatively little attention being directed at the isomorphous PrFeB system [5]. The $Pr_2Fe_{14}B$ phase has two advantages over $Nd_2Fe_{14}B$ [8] in that its anisotropy field H_a is larger and it does not undergo a spin reorientation at low temperatures, although, on the other hand, it has a slightly lower Curie temperature T_C and is more costly. The larger H_a of the $Pr_2Fe_{14}B$ gives the potential for an increased intrinsic coercivity ${}_jH_c$ and this has particular relevance for the nanocrystalline materials which are subject to marked attenuation of coercivity as a corollary of remanence enhancement.

This paper summarises the results of a systematic study of the influence of $Pr_2Fe_{14}B$ grain size d_g (generally below 40 nm) and of Pr/Fe ratio on the coercivity and remanence of a series of $Pr_xFe_{94-x}B_6$ alloys with x varying between 6 and 20 at%. The magnetic properties are compared with those of corresponding nanophase NdFeB alloys studied earlier at Sheffield [6] and discussed in terms of the microstructure and phase constitution, and of the respective anisotropy fields for the two 2/14/1 phases.

2. Experimental procedures

A series of $Pr_xFe_{94-x}B_6$ alloys with x varying from 6 to 20 at% was prepared by co-melting the pure constituents in an argon arc melting unit. The cast alloys were then chill block melt spun under an argon atmosphere at various roll speeds v_r in the range 14 to 22 $m\,s^{-1}$. The ribbon thicknesses were typically in the range 20–60 μm. The roll speed influenced the microstructure, notably the $Pr_2Fe_{14}B$ crystallite size d_g (d_g varying inversely with v_r), which, in turn, had a marked effect on the magnetic properties for each alloy. The values of d_g for the $Pr_2Fe_{14}B$ phase were determined by X-ray diffraction (XRD) line broadening analysis of non-overlapping diffraction peaks [9] and the distribution and size of primary and second phase particles for selected alloys were also studied using transmission electron microscopy (TEM). The XRD and TEM data

*Corresponding author.

0925-8388/98/$ – see front matter
PII: S0925-8388(98)00763-4

indicated that the crystallites were randomly oriented. The magnetic properties of individual pieces of ribbon were measured using a vibrating sample magnetometer coupled to a superconducting magnet having a maximum applied field of 5 T. The ribbons were magnetised across their width, so that no corrections for self-demagnetisation were needed.

3. Results and discussion

3.1. Effect of mean crystallite size on the magnetic properties of PrFeB-based alloys

The series of alloys was divided into three groups: low Pr, near-stoichiometric and high-Pr alloys, corresponding to Pr contents of 6–10, 12 and 14–20 at% Pr, respectively. Microstructural analysis using XRD and TEM showed that the first group is comprised of a mixture of soft magnetic α-Fe grains and the hard $Pr_2Fe_{14}B$ magnetic phase. The near-stoichiometric alloy was found to be single phase, though very small amounts of a second phase at triple points were sometimes observed by TEM. The third group was comprised of $Pr_2Fe_{14}B$ crystallites surrounded by a Pr-rich paramagnetic phase which partly isolates and decouples the hard grains.

The dependence of the intrinsic coercivity $_jH_c$, and remanent polarisation J_r and the maximum energy product $(BH)_{max}$ on mean crystallite size, d_g, for the four low-Pr alloys is shown in Fig. 1. The data are plotted for the roll-contact surfaces of the ribbons and the dependencies on d_g are very similar to those for the non-contact surfaces, the difference being the somewhat larger d_g obtained for the latter.

The coercivity in each case tends to increase initially with decreasing d_g up to a maximum value and then subsequently decreases with further decrease in d_g. This latter decreases was identified by XRD with the onset of vitrification. The value of the maximum $_jH_c$ tends to decrease with diminishing Pr content, although the data for the 9 and 10 at% Pr alloys are reversed. The attenuation of $_jH_c$ for Pr contents below 9 at% is rapid, as the volume fraction of the α-Fe phase increases (up to ~50% at 6 at% Pr, since the solubility of Pr in α-Fe is small, $\ll 1$ at%). The remanence J_r, as expected, decreased as d_g becomes increasingly refined, up to a maximum in each case, corresponding to a critical $Pr_2Fe_{14}B$ grain size below which vitrification is initiated. The J_r is in all cases enhanced well above the expected value for single phase, randomly oriented $Pr_2Fe_{14}B$ (0.79 T) [8], although the range of d_g covered in each case only is 10 nm or less. The enhancement is considered to be the result both of a nanoscale structure and of the presence of the α-Fe (Fig. 2), whose saturation polarisation J_s, 2.2 T, is substantially greater than that of $Pr_2Fe_{14}B$ (1.58 T). This is discussed later. The maximum J_r tends to increase with decreasing Pr

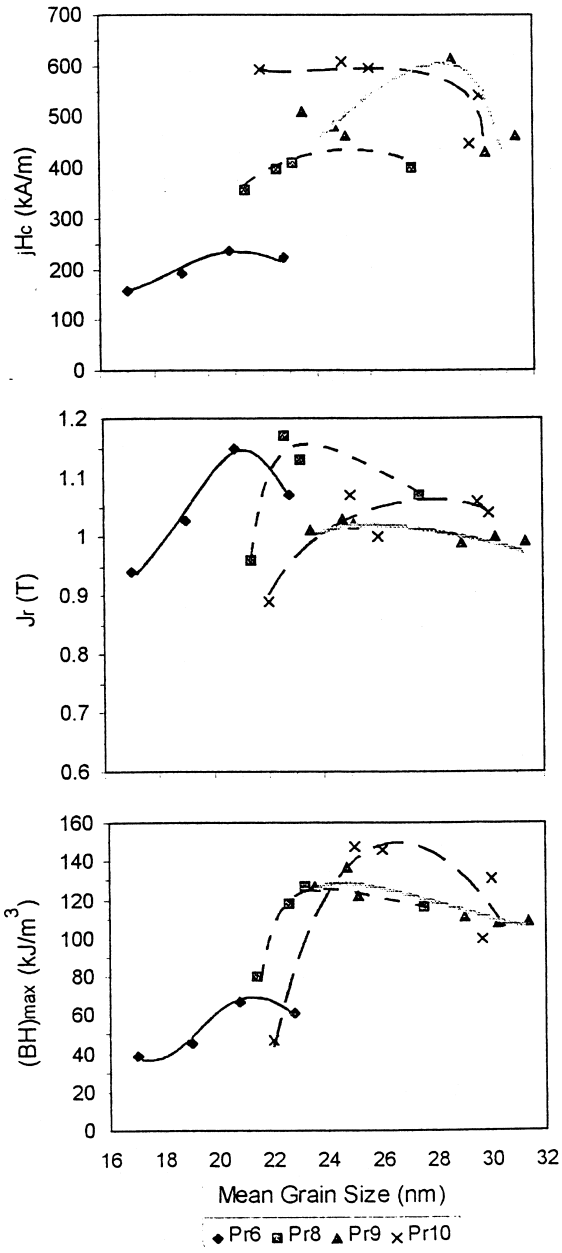

Fig. 1. Magnetic properties vs. mean $Pr_2Fe_{14}B$ crystallite size d_g for substoichiometric Pr alloys.

content, reflecting largely the increasing volume fraction of α-Fe. However, there may also be an effect arising from the fact that d_g corresponding to the maximum J_r is decreasing with Pr content (i.e., greater exchange enhancement in the $Pr_2Fe_{14}B$ crystallites), athough, in any case, d_g would tend to decrease because the volume fraction of the hard magnetic phase diminishes as the Pr content is lowered. The maxima occur roughly at the same d_g as the maxima in $_jH_c$.

The dependence of $(BH)_{max}$ on d_g for each alloy largely parallels that for the respective J_r, as would be expected, since, generally, the magnitude of $(BH)_{max}$ is dominated

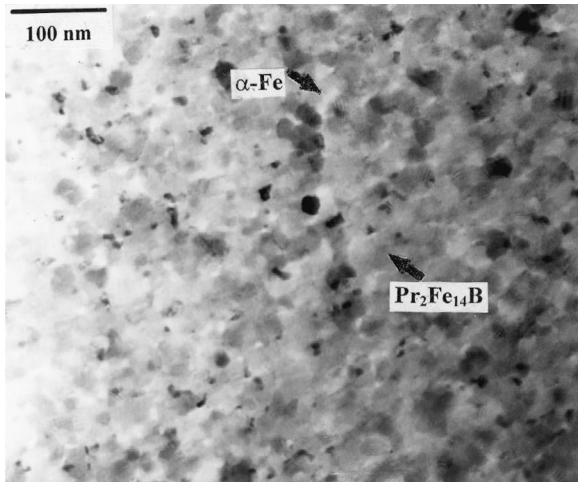

Fig. 2. TEM micrograph of a $Pr_{10}Fe_{84}B_6$ alloy melt-spun at 18 m s^{-1} showing $Pr_2Fe_{14}B/\alpha$-Fe nanocomposite structure.

by J_r. Thus, the high values, up to 150 kJ m^{-3}, are symptomatic of substantial exchange enhancement. However, $(BH)_{max}$ for the 6 at% Pr alloy is markedly attenuated, in spite of the high J_r, because of the very low $_jH_c$ which results in a non-linear B–H second quadrant characteristic [10].

For the near-stoichiometric 12 at% Pr alloy $_jH_c$, in contrast to the low-Pr alloys, has a high value (~1600 kA m^{-1}) at the largest d_g (~43 nm) and decreases continuously as d_g is reduced (Fig. 3). The remanence increases to a maximum of ~0.96 T at a surprisingly high d_g (~37 nm) below which vitrification sets in. Thus, in this case, $_jH_c$ is diminished as J_r is enhanced as was shown for a single phase NdFeBSi alloy [2]. The enhancement of J_r is smaller than for the low-Pr alloys due to the absence of α-Fe nanocrystallites (i.e., lower effective J_r for the alloy) and probably also to the fact that d_g at peak J_r is significantly greater than for the nanocomposite alloys.

The behaviour of the high-Pr alloys in terms of dependence of magnetic properties on d_g (Fig. 4) is qualitatively similar to that for the substoichiometric alloys in Fig. 1, with $_jH_c$ and J_r achieving maxima at critical values of d_g which generally increase with enhancing Pr content. The peak values of $_jH_c$ are, however, substantially larger in this case, up to ~2000 kA m^{-1}, and increase somewhat as the Pr concentration is enhanced. Apart from the 14 at% Pr alloy, J_r is in all cases <0.79 T (i.e., $J_s/2$), which reflects a combination of the effect of volume dilution of the $Pr_2Fe_{14}B$ crystallites and a partial decoupling of the $Pr_2Fe_{14}B$ crystallites by the paramagnetic rich Pr-phase located at the grain boundaries (Fig. 5). Clearly, this layer becomes more effective as its volume fraction is enhanced with increasing Pr content. That this layer is only partly isolating the $Pr_2Fe_{14}B$ grains is illustrated by the fact that the maximum J_r for the 14 at% Pr alloy is 0.86 T, which is consistent with some exchange enhancement above the

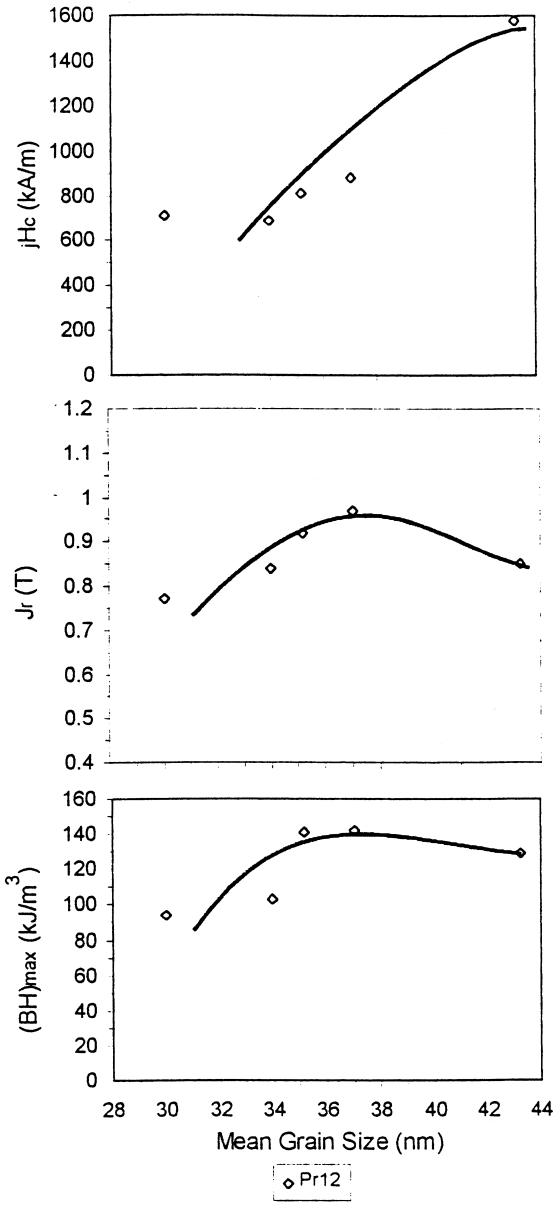

Fig. 3. Magnetic properties vs. d_g for near-stoichiometric $Pr_{12}Fe_{82}B_6$ alloy.

Stoner–Wohlfarth value of 0.79 T. The $(BH)_{max}$ values are generally attenuated in consonance with the lowered J_r but, again, the peak value for the 14 at% Pr sample is usefully high at ~130 kJ m^{-3}.

Typical J–H loops for the three classes of nanophase alloys are shown in Fig. 6 which emphasise that the increased enhancement of J_r as the Pr content is decreased is at the expense of $_jH_c$ [6].

The influence of Pr content on d_g for various roll speeds is shown in Fig. 7. In each case where the data span the whole range of Pr concentration, d_g passes through a maximum at 12 at% Pr. This probably, at least partly, reflects the fact that the volume fraction of the $Pr_2Fe_{14}B$ decreases with increasing departure from the stoichio-

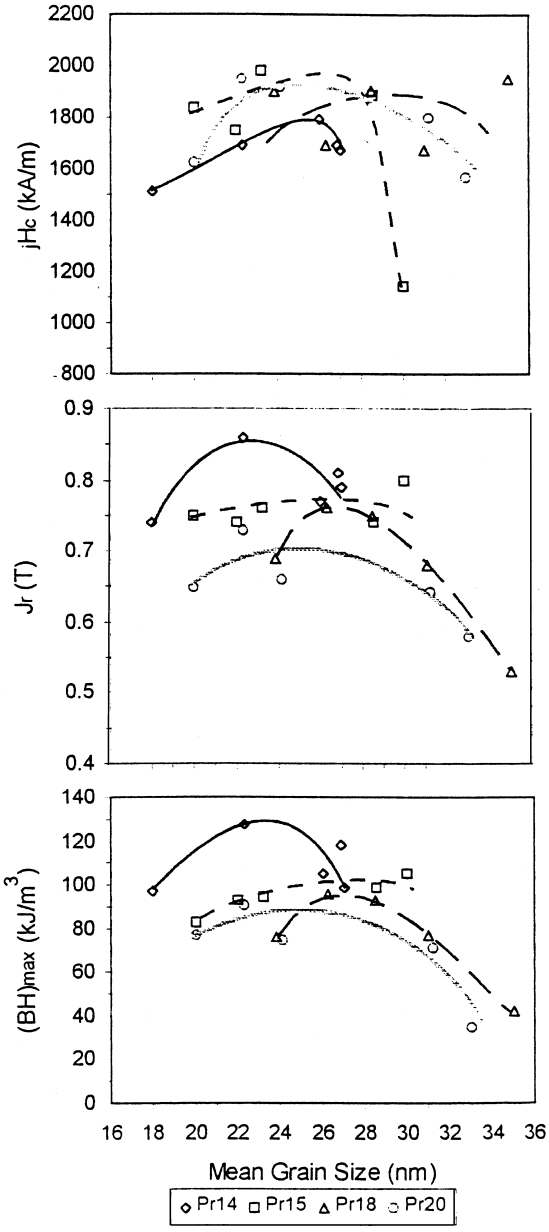

Fig. 4. Magnetic properties vs. d_g for high-Pr alloys.

metric composition, in either direction. The fact that the decline in d_g with at% Pr on the low Pr side is steeper than on the high Pr side is consistent with this since the volume fraction of the α-Fe phase should be approximately proportional to $(12-x)$, where x is at% Pr in the alloy, whereas the volume fraction of the Pr-rich phase (the corresponding phase for NdFeB has the formula $Nd_{73}B_{27}$) is still relatively small even at $x=20$ at%. However, it was noted that the lower Pr alloys (6–8 at%) quenched to a partly amorphous structure at surprisingly large thicknesses (~50 μm), indicating a higher glass forming ability than for the higher Pr compositions. This factor would also contribute to the steep decrease of d_g for the substoichiometric alloys.

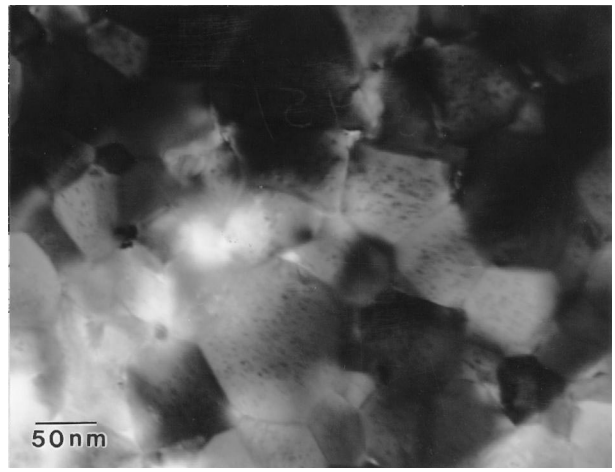

Fig. 5. Microstructure of a $Pr_{15}Fe_{79}B_6$ alloy showing $Pr_2Fe_{14}B$ grains and intergranular Pr-rich phase.

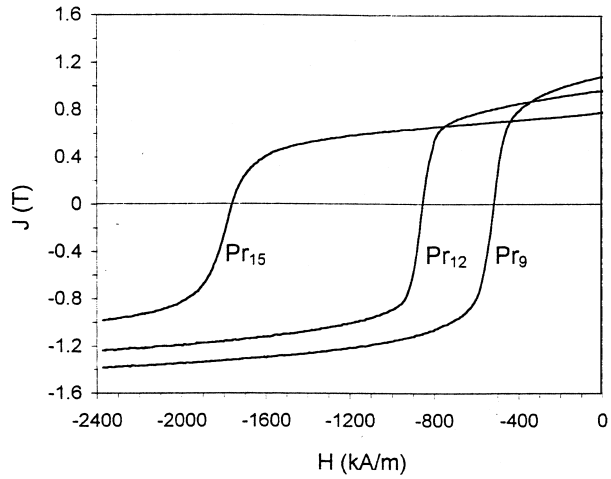

Fig. 6. Parts of typical hysteresis loops for three contrasting Pr compositions.

3.2. Effect of Pr/Fe ratio on the magnetic properties and comparison with NdFeB alloys

The dependence of the magnetic properties of $Pr_xFe_{94-x}B_6$ ribbons (for d_g corresponding to the maxi-

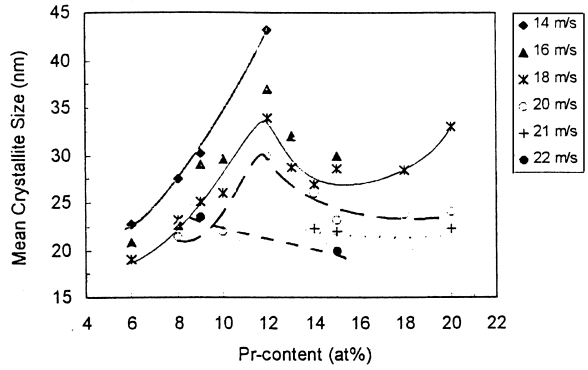

Fig. 7. Effect of Pr content on d_g at different roll speeds.

mum J_r in each case) on Pr concentration x within the range 6–20 at% is shown in Fig. 8. Also shown for comparison is the corresponding plot for $Nd_xFe_{94-x}B_6$ ribbons (for d_g 25–30 nm), in this case for x within the range 8–19 at%. This shows clearly that the intrinsic coercivity, apart from the 8 at% RE alloy, is systematically larger for the Pr series than for the Nd series with the difference increasing to a maximum of ~400 kA m^{-1} (allowing for the experimental scatter) at 14 at% RE. The remanent polarisation J_r is also slightly larger for the Pr system for RE ≤13 at% (although the values are virtually identical for larger x) and the deviation increases progressively down to 8 at% RE, the limit of measurements for the Nd system. The value of J_r rises continuously with decreasing x for both systems and exceeds 1.25 T at $x=6$ at% for the Pr system. The larger J_r is also carried through to a larger $(BH)_{max}$ for $x>8$ at%, for the Pr system. However, as indicated in the previous section and discussed previously [10], the benefit in increased $(BH)_{max}$ arising from enhanced J_r is limited by the diminishing $_jH_c$ at very low RE content so that the corresponding $(BH)_{max}$ drops rapidly as a result of a non-linear second quadrant $B–H$ characteristic.

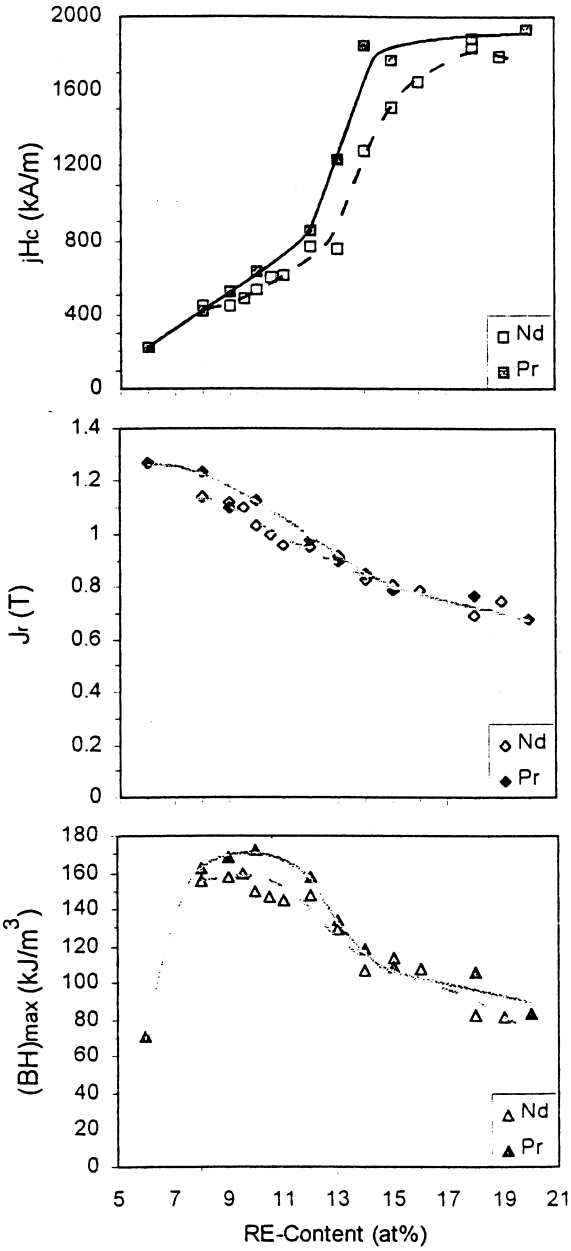

Fig. 8. Effect of rare-earth content on the magnetic properties for ribbons comprised of crystallites with d_g~20–30 nm for PrFeB and d_g~25–30 nm for NdFeB.

The exchange constant A is very similar for the two 2/14/1 phases while H_a at 300 K is some 30% larger for the $Pr_2Fe_{14}B$ [8]. Thus, it would be expected that the exchange length for the $Pr_2Fe_{14}B$ phase would be approximately 15% smaller than for $Nd_2Fe_{14}B$ (which is about 4 nm) since $L_e \propto \sqrt{A/K}$, where K is the exchange constant. The enhancement of J_r above the Stoner–Wohlfarth value [11] of 0.79 T at small d_g for the near-stoichiometric composition $Pr_{12}Fe_{82}B_6$ is due to exchange coupling between 2/14/1 unit cells in neighbouring crystallites which extends over a length L_e. The effect on J_r should become noticeable when d_g is such that the exchange volume in unfavourably oriented crystallites, with respect to the magnetising direction, becomes a significant fraction of the grain volume.

For the $Nd_2Fe_{14}B$ alloy (with a minor amount of silicon dopant), the critical d_g was found to be approximately 40 nm [1]. In the present case for the stoichiometric $Pr_2Fe_{14}B$ alloy, there are insufficient data points to enable an estimate to be made of the critical d_g nor can a judgement be made for the low-Pr nanocomposite alloys since the experimental scatter is also rather large. Nevertheless, it is interesting to observe that the degree of J_r enhancement for a similar d_g is virtually identical for the two stoichiometric alloys. The larger enhancement for the PrFeB system at low RE contents can be ascribed to a progressively smaller reference d_g with decreasing Pr, whereas the reference d_g was roughly constant at 25–30 nm in the case of the NdFeB data. As has been noted previously, the increasing J_r with diminishing x can be ascribed to a progressively increasing volume fraction of soft magnetic α-Fe phase. The 2/14/1 crystallites exchange couple also to the α-Fe grains [3,6] and since L_e is substantially larger (~35 nm) for the latter than for the former and the α-Fe crystallites are smaller than the $Pr_2Fe_{14}B$ grains, all the moments in the α-Fe grains are aligned parallel by the exchange process.

The systematically higher $_jH_c$ for the PrFeB alloys is consistent with the 30% larger H_a for the $Pr_2Fe_{14}B$ [8] (at least up to 15 at% RE). However, the overall shape of the $_jH_c–x$ relationship is broadly similar in the two systems with a roughly linear decrease below $x=12$ at% RE, reflecting the increasing volume fraction of the α-Fe phase which, although it contributes to further J_r enhancement, would be expected to reduce the effective overall H_a.

Between 12 and ~15 at % RE, the rate of increase of $_jH_c$ with x accelerates in both systems, evidently due to the presence of an increasing fraction of the paramagnetic RE-rich phase ($Nd_{73}Fe_{27}$ for the NdFeB system) which tends to decouple the $RE_2Fe_{14}B$ crystallites. However, it is not clear why the rate of increase of $_jH_c$ levels off at high RE (very sharply at ~15 at% Pr in the case of the PrFeB system).

It is evident from the present data that the nanophase PrFeB melt spun alloys give significantly better overall combinations of magnetic properties for a given mean diameter of the 2/14/1 crystallites and, between ~9 and 12 at% Pr, excellent combinations of $(BH)_{max}$ and $_jH_c$ are obtained. This has significant implications for the exploitation of the nanophase ribbon in polymer bonded magnets for technological applications, since the nanocomposite NdFeB alloys, especially, tend to have rather low coercivities.

4. Conclusions

The mean $Pr_2Fe_{14}B$ crystallite size within the nanocrystalline range has a marked effect on the magnetic properties for all the alloy compositions studied. In general, grain refinement below ~35 nm causes all the magnetic properties to be enhanced until amorphisation intervenes, the exception being the near-stoichiometric alloy $Pr_{12}Fe_{82}B$ for which $_jH_c$ diminishes as J_r is exchange enhanced.

Excellent combinations of $_jH_c$ and $(BH)_{max}$ were observed for Pr in the range 9–12 at%, and the system appears to offer clear advantage over corresponding nanophase NdFeB alloys in having significantly higher $_jH_c$ (up to 30% better) for a given enhancement of $(BH)_{max}$. This is considered to result from the larger anisotropy constant for the $Pr_2Fe_{14}B$ phase.

Acknowledgements

G.M. acknowledges the award of a research studentship from CONACYT (Mexico) and H.A.D. is grateful to the Engineering and Physical Sciences Research Council for the support of his research in this field.

References

[1] J.E. Keem, G.B. Clemente, A.M. Kadin, R.W. McCallum, in: J.A. Salsgiver (Ed.), Hard and Soft Magnetic Materials and Applications Including Superconductivity, Proceedings of a Conference ASM Materials Week 87, American Society for Metals, 1987, p. 87.
[2] A. Manaf, R.A. Buckley, H.A. Davies, M. Leonowicz, J. Magn. Magn. Mater. 101 (1991) 360.
[3] R. Coehoorn, D.B. De Mooij, J.P.W.B. Duchateau, K.H.J. Buschow, J. Phys. 49 (1988) C8.
[4] A. Manaf, R.A. Buckley, H.A. Davies, J. Magn. Magn. Mater. 128 (1993) 302.
[5] J. Ding, P.G. McCormick, R. Street, J. Magn. Magn. Mater. 124 (1993) 1.
[6] H.A. Davies, J. Magn. Magn. Mater. 157–158 (1996) 11.
[7] T. Schrefl, J. Fidler, H. Kronmuller, Phys. Rev. B 49 (1994) 49.
[8] S. Hirosawa, Y. Matsuura, H. Yamamoto, S. Fujimura, M. Sagawa, H. Yamauchi, J. Appl. Phys. 59 (1986) 873.
[9] G.E. Carr, H.A. Davies, R.A. Buckley, Mater. Sci. Eng. 99 (1988) 147.
[10] A. Manaf, P.Z. Zhang, I. Ahmad, H.A. Davies, R.A. Buckley, IEEE Trans. Magn. 29 (1993) 2866.
[11] E.C. Stoner, E.P. Wohlfarth, Philos. Trans. R. Soc. A 240 (1948) 599.